Letter

First measurement of neutron birefringence in polarized ^{129}Xe and ^{131}Xe nuclei

H. Lu [1], M. J. Barlow [2], D. Basler [3], P. Gutfreund [4], O. Holderer [5], A. Ioffe [5], S. Pasini [5], P. Pistel [6], Z. Salhi [5], K. Zhernenkov [5], B. M. Goodson [3], W. M. Snow [1], and E. Babcock [5,*]

[1] *Indiana University/CEEM, 2401 Milo B. Sampson Lane, Bloomington, Indiana 47408, USA*

[2] *School of Medicine, University of Nottingham, Queens Medical Centre, Nottingham NG7 2RD, United Kingdom*

[3] *School of Chemical and Biomolecular Sciences, Southern Illinois University, Carbondale, Illinois 62901, USA*

[4] *Instut Laue-Langevin, 71 Avenue des Martyrs, CS 20156, 38042 Grenoble Cedex 9, France*

[5] *Forschungszentrum Jülich GmbH, Jülich Centre for Neutron Science (JCNS) at Heinz Maier-Leibnitz Zentrum (MLZ), 85747 Garching, Germany*

[6] *Forschungzentrum Jülich mbH, ZEA-1, 52425 Jülich, Germany*

(Received 31 December 2022; revised 27 July 2023; accepted 17 November 2023; published 4 January 2024)

We present measurements of polarized neutron birefringence in transmission through nuclear-polarized ^{129}Xe and ^{131}Xe gas and determine the neutron incoherent scattering lengths $b_i(^{129}\mathrm{Xe}) = -0.186 \pm (0.021)_{\mathrm{stat.}} \pm (0.004)_{\mathrm{syst.}}$ fm and $b_i(^{131}\mathrm{Xe}) = 2.09 \pm (0.29)_{\mathrm{stat.}} \pm (0.12)_{\mathrm{syst.}}$ fm. These results determine the essential parameter needed for interpretation of spin-dependent neutron-scattering studies on polarized xenon ensembles with possible future applications ranging from tests of time-reversal violation to mode-entangled neutron scattering experiments on nuclear-polarized systems.

DOI: 10.1103/PhysRevC.109.L011001

This work presents the measurement of neutron birefringence in polarized ^{129}Xe and ^{131}Xe nuclei, which gives the nuclear polarization-dependent bound scattering length difference $\Delta b = b_+ - b_-$ for nuclear spin I parallel or antiparallel to the neutron spin s. Knowing Δb one can now conduct and interpret spin-dependent neutron scattering from an ensemble of polarized xenon nuclei using the well-established theory of Van Hove [1,2] generalized for neutron spin-dependent scattering from polarized nuclei [3]. Because nuclear-polarized xenon ensembles can be created in conditions where the electron spins do not dominate the magnetic properties (unlike the great majority of magnetic systems in condensed matter), our work enables qualitative types of polarized neutron investigations. Highly polarized ensembles of xenon gas can be created by spin-exchange optical pumping (SEOP) [4–12] in volumes high enough to create long-lived polarized Xe liquids and solids by freezing [13–15] for exploration of subtle properties of these "pure" spin systems. The conclusion of this paper describes examples of possible future polarized neutron investigations that make essential use of the special properties of polarized xenon in quantum entanglement [16,17] and in searches for new sources of time reversal violation. These newly enabled neutron scientific applications of polarized ^{129}Xe and ^{131}Xe can also complement their many existing applications in biomedical imaging [4,10,12,18–21], nuclear magnetic resonance (NMR) spectroscopy [18,22], fluid dynamics [18,20,22], gas/surface interactions [23–25], studies of Berry geometric phases [26], and searches for charge parity time (CPT) symmetry and/or Lorentz violation [27–32], electric dipole moments [33,34], and axion-like particles [35,36].

Neutron scattering amplitudes are often expressed in operator form as $b = b_c + b_i \vec{s} \cdot \vec{I}$, where $\vec{s}$ is the neutron spin, $b_c = [(I+1)b_+ + Ib_-]/(2I+1)$ is the spin-independent coherent scattering length, and the spin-dependent incoherent scattering length $b_i = I\sqrt{I+1}[b_+ - b_-]/(2I+1)$ is directly proportional to Δb. For ^{129}Xe or ^{3}He with nuclear spin $I = \frac{1}{2}$ the compound neutron-nucleus total spin $J = I \pm s$ can form a triplet ($J = 1$) and singlet ($J = 0$) total spin state corresponding to the $b_1 \equiv b_+$ and $b_0 \equiv b_-$ channels, so $\Delta b = b_1 - b_0$. For $I = \frac{3}{2}$ ^{131}Xe, $m_J = 2, 1, 0, -1$ are possible. Δb measures the difference of the $b_{m_J=2} + b_{m_J=1}$ and $b_{m_J=0} + b_{m_J=-1}$ scattering amplitudes for spin order characterized by the nuclear polarization $P_x = \langle I_z \rangle / I$ with no tensor alignment. A general analysis of neutron spin dynamics in media with nuclear spin order [37] implies that, for the precision reached here and for the neutron energies far from neutron-nucleus resonances used in this work, we can relate the spin rotation angle to the scattering length difference in the usual way. Texts on neutron optics [38] discuss the statistical weight factors used to derive the above relations.

We measured Δb by observing the change in phase of the neutron spin as neutrons pass through a polarized nuclear target, a method referred to as "pseudomagnetic precession" [39]. Although this phenomenon was initially described [39,40] in terms of a fictitious "pseudomagnetic field" inside the sample, Δb originates from neutron-nucleus scattering.

*e.babcock@fz-juelich.de

The optical theorem [38] relates the spin dependence of the neutron optical potentials associated with the scattering amplitudes b_+ and b_- to a two-valued neutron index of refraction (n_+, n_-) depending on the relative orientation of the neutron spin and the nuclear polarization:

$$n_\pm^2 = 1 - \frac{4\pi}{k^2} N(b_{\rm coh} + b_\pm),$$
$$\Delta n = (n_+ - n_-) \approx -\frac{2\pi}{k^2} N(b_+ - b_-), \tag{1}$$

where N is the number of nuclei per unit volume, k is the neutron wave number, and the approximation in the second expression is valid in our case as the neutron index of refraction is $\simeq 1$. Δn makes the medium optically birefringent for neutrons so that the two helicity components of the neutron spin state accumulate different phases, $kn_\pm d$, in the forward direction as neutrons propagate a distance d through the target. Therefore neutron spins orthogonal to the nuclear polarization direction of the target precess around the nuclear polarization by an angle $\phi^* = k\Delta n d$. Many texts and reviews on neutron optics state that the birefringence experienced by neutrons in magnetized media is a direct consequence of the two-valued neutron index of refraction and leads to analogous effects as in light optics [41–43]. It is perhaps conceptually important to point out that neutrons, unlike light photons whose quantization axis is defined by their direction of motion, have a quantization axis defined by the magnetic field direction, i.e., the polarization axis, which can be arbitrary with respect to the neutrons' direction of propagation. Thus the neutron birefringence is expressed in the plane perpendicular to the magnetic field as opposed to the direction of motion for light.

Measurements of neutron birefringence are well suited to the Ramsey method of separated oscillatory fields [44,45]. Previous work [40,46–49] determined Δb for several nuclei dynamically polarized in the solid state. We used the neutron spin-echo (NSE) technique [50] to measure Δb in SEOP cells filled with ^{3}He, ^{129}Xe, or ^{131}Xe (an earlier measurement in ^{3}He [51] also used this method). The measurement sequence is similar to spin echo manipulations in nuclear magnetic resonance [52], however the precession and flipping fields are encountered in space along the traveling neutron beam, as opposed to time-dependent fields applied to spins at rest in the laboratory frame. In contrast to the Ramsey sequence, NSE uses a π spin flip at the field symmetry point (Fig. 1) to refocus the spin precession of neutrons with different velocities so they are rephased at the polarization analyzer. Phase shifts of the interference fringes from the sample are compensated by DC magnetic fields from phase (compensation) coils, which are scanned over several periods about the compensation point to obtain the NSE signal. The sensitivity of the measurement is therefore set by the ratio of the field resolution in the compensation coils to the total field integral of the instrument. Since for the J-NSE instrument [53] used in this work the phase coil precision can be nT/m compared to a total field integral on the instrument of over 1 T/m, very high phase precision is possible.

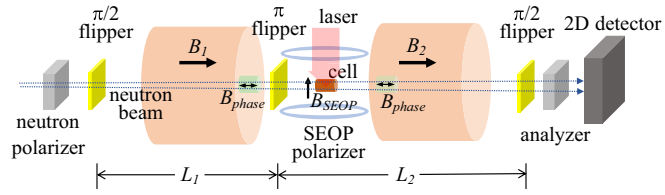

FIG. 1. A schematic drawing of a NSE instrument following the description in the text. The first neutron $\pi/2$ flipper sets the neutron spins to precess about the total field defined by the direction of B_1, $B_{\rm SEOP}$, or B_2, i.e., in the respective regions. The π flipper reverses neutron precession and the second $\pi/2$ flipper and analyzer return the in-phase magnitude of the final neutron polarization.

The spin-echo condition holds for any group of neutron velocities at $B_{1,\rm echo} = \frac{L_2}{L_1} B_2$, where the number of forward precessions though field B_1 over length L_1 in the first region and back precessions in the second region of field B_2 and length L_2 are equal, i.e., $\phi_1(B_{1,\rm echo}) = \phi_2$. The phase shift accumulated in either region is $\frac{\gamma m \lambda}{2\pi\hbar} B_1 L_1$ where m is the mass of a neutron with de Broglie wavelength λ and gyromagnetic ratio γ. The additional phase shift from Δb modifies the spin echo condition by adding an extra phase ϕ^*. The precession caused by the neutron birefringence is

$$\phi^* = -\frac{2I}{2I+1} \lambda P_x N_x d_x \Delta b^x$$
$$= -2\sqrt{\frac{I_x}{I_x+1}} \lambda P_x N_x d_x b_i^x. \tag{2}$$

Here, $I_3 = I_{129} = 1/2$ for ^{3}He and ^{129}Xe and $I_{131} = 3/2$ for ^{131}Xe, and P_x and N_x are the polarization and number density of the respective polarized nuclei of atomic weight x with corresponding scattering length difference Δb_i^x or incoherent scattering length b_i^x. The relevant product $P_x N_x$ is determined by NMR calibration measurements using absolute $P_3 N_3$ of the ^{3}He cell from neutron transmission as a standard. ϕ^* is then measured from the shift of the NSE signal upon reversal of the nuclear polarization with all static magnetic fields constant. Whereas the classical NSE used here senses precession, incoherent scattering lengths can equivalently be measured by the techniques of intensity-modulated NSE [54]—or the even the MIEZE technique in neutron resonant spin echo [55]—where the neutron does not experience precession while it is interacting with the sample (and is even unpolarized in the latter), showing the necessity of scattering theory and the optical theorem to describe the effect.

Figure 1 shows the self-compensated superconducting (SC) coil sets for the two precession regions of the J-NSE [56]. The polarized noble gas samples rest in the sample region inside a B_0 holding field normal to the neutron beam. Three GE180 SEOP cells [57] produced in FZ-Jülich were used in this experiment. The ^{3}He and ^{129}Xe cells were prepared in Garching (FZ-Jülich) [58] and the ^{131}Xe cell was prepared and characterized at Southern Illinois University [59].

Two frequency-narrowed diode array bars [60] realized *in situ* SEOP. A 70 cm diameter Helmholtz coil pair produced the magnetic field $B_{\rm SEOP}$ normal to the neutron path. Cell

TABLE I. The relative error contributions divided between systematic and statistical sources. The statistical error of the ϕ measurement dominates. The estimate of $\sigma_1 = 24$ barn from [62,67] was used; the - denotes a one-sided systematic that would lower the reported b_i values.

isotope	^{129}Xe	^{131}Xe
δb_i	**0.112**	**0.150**
δb_i stat.	**0.110**	**0.139**
stat. error source		
$\delta\phi$	0.106	0.118
$\frac{\delta}{\delta R}(\cosh^{-1}(R))$	0.0057	0.0057
$\delta(S_3/S_{129})$	0.028	0.028
$\delta(S'_{129}/S'_{131})$		0.067
δb_i syst.	**0.023**	**0.055**
syst. error source		
σ_1	−0.0045	−0.0045
δd_3	0.021	0.021
δd_{129} or δd_{131}	0.0079	0.0079
repeatability Xe pol.		0.05

heating and temperature regulation was provided by AC electric cartridge heaters for the ^{3}He cell and by flowing air for the two xenon cells. NMR free-induction decay (FID) measurements of the cell magnetizations (P_xN_x) used a home-built pulse-receive system [60]. Since the three isotopes studied here vary in gyromagnetic ratios $\gamma/2\pi = \gamma'$ by an order of magnitude ($\gamma'_3 = -3.243$ kHz/G, $\gamma'_{129} = -1.178$ kHz/G, and $\gamma'_{131} = 0.349$ kHz/G for ^{3}He, ^{129}Xe, and ^{131}Xe, respectively), the NMR FID calibrations presented an experimental challenge.

The ratio $R = T_p/T_0$ of the neutron transmission through the polarized (T_p) to unpolarized (T_0) ^{3}He cell determines

$$\cosh^{-1}(R) = \frac{\sigma*}{\lambda_{th}}\lambda P_3 N_3 d_3, \tag{3}$$

where $\sigma* \simeq \sigma_{un} = 5333(7)$ barn is the ^{3}He unpolarized neutron absorption cross section normally used to characterize neutron properties of ^{3}He neutron spin filter cells [61], $\lambda_{th.} = 1.798$ Å is the standard reference wavelength for thermal neutron cross sections, and λ the neutron wavelength used. Note the polarized ^{3}He neutron absorption cross section, $\sigma* = \sigma_p = \sigma_{un} - \sigma_1$ should actually be used to characterize P_3. Here, σ_1 is the ^{3}He neutron triplet state absorption cross section which is estimated to be 24 barn [62]. σ_1 is not well known resulting in the small systematic error in the value of P_3, given in Table I (also see the Appendix). $P_3N_3 = 0.609 \pm 0.145 \times 10^{24}$ m^{-3} was obtained directly from the mean intensity of the NSE curves for the polarized and unpolarized ^{3}He cell through the cell center where $d_3 = 4.8 \pm 0.1$ cm. Separate neutron transmission measurements through different parts of the ^{3}He cell using neutron time of flight [63,64] determined $N_3 = 8.627 \pm 0.027 \times 10^{24}$ m^{-3} and characterized the path length through its somewhat rounded ends. d_3 is inferred from measurements of the cell's external length and assumptions of the glass thickness resulting in the given error. This density implies $P_3 = 70.6 \pm 1.6\%$. Only the product P_3N_3 is needed for absolute NMR calibration, but the Xe cell lengths are needed to solve for Δb of ^{129}Xe and ^{131}Xe. The NSE profiles of the transmitted neutrons were fit in the usual way to determine ϕ for each pixel of the two-dimensional (2D) detector [56].

The data were taken in defined time-ordered sequences of alternating up and down target polarizations for all three nuclei. Since the incoherent scattering length b_i^3 of ^{3}He has been measured previously [51] and was known to be large compared to our expected effects in ^{129}Xe and ^{131}Xe, we used these data to check the experimental procedure and apparatus. The up/down polarization states for the polarized xenon targets were switched by reversing the pump-laser polarization by turning the quarter-wave plates without any other changes. The nuclear polarization is reversed by SEOP on a timescale near the T_1 relaxation time of ^{129}Xe, about 5 min for our cell, so one 20 min NSE scan was skipped after each wave plate change. For ^{131}Xe, $T_1 \simeq 30$ s [59,65] is much shorter than the scan time and the polarization buildup time is negligible. It is assumed the polarization reversal was symmetric within measurement errors.

We analyzed the individual NSE scans in single detector pixels for each run. The spin echo stationary phase point varies slightly across the neutron beam due to the small spatial variations in the field integral, and the spin echo phase drifts slowly over timescales long compared to the target spin flip due to very small changes in the total field over time. To improve the signal/noise ratio for fitting the pixel spin echo scans, we applied a fast Fourier transform (FFT) frequency filter to the spin echo data. The precession angle is extracted from the relative phase shift between oppositely polarized nuclear target states with the NSE scans performed using alternating groups of polarizations. A further discussion of the NSE data analysis for this work is given in [66]. The absolute phase ϕ was well represented by a square wave on top of a slowly varying linear instrumental phase drift (Fig. 2). This analysis resulted in precession angles averaged over the active detector pixels of $4.05^\circ \pm 0.43^\circ$ for the ^{129}Xe target and $3.05^\circ \pm 0.36^\circ$ for the ^{131}Xe target.

We then use Eq. (2) to compute the incoherent scattering lengths b_i. Since the NMR calibration of the Xe measures magnetization proportional to P_xN_x, any error in N_x for Xe drops out for the determination of b_i. Using the NMR calibrations, we determine P_xN_x for the two xenon isotopes as follows. For $I = 1/2$ ^{129}Xe and ^{3}He and for NMR FID performed in the very low tip angle limit (i.e., $\ll 90^\circ$),

$$P_{129}N_{129} = P_3N_3\left(\frac{\gamma_3}{\gamma_{129}}\right)^2\frac{S_{129}V_3}{S_3V_{129}}, \tag{4}$$

where the ratio of gyromagnetic ratios is squared to scale for both the coil pickup and tipping pulse at fixed tip parameters, S_x is the NMR strength of the respective noble gas isotope and $V_{129}/V_3 = 4.085$ was the increase in tip amplitude for ^{129}Xe to obtain a good signal/noise ratio (S/N). Using this relation $P_{129}N_{129} = 1.62 \pm 0.04 \times 10^{24}$ m^{-3}. The 0.3 bar total Xe pressure measured during cell filling implies $P_{129} = 17.6\%$.

The ^{131}Xe NMR calibration could not be performed during the neutron experiment with our standard pickup coil as the lower ^{131}Xe polarization and the small ^{131}Xe

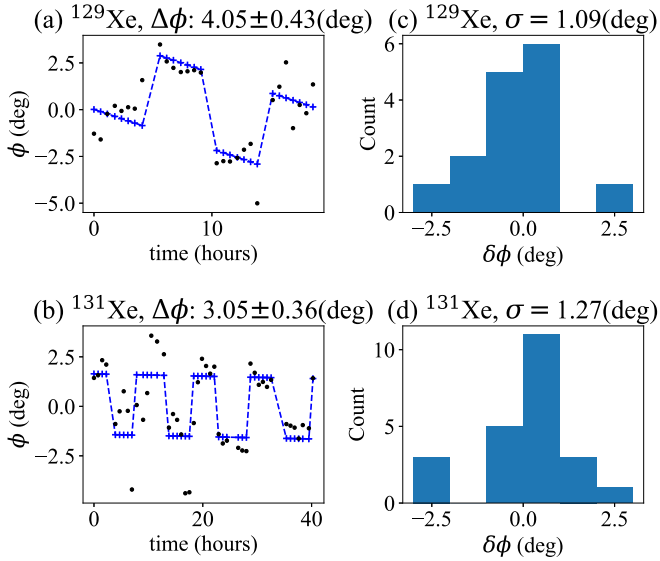

FIG. 2. (a), (b) Plots of relative NSE phases of ^{129}Xe and ^{131}Xe versus experiment time. Black dots are data and the blue crosses are the model to extract $\Delta\phi$, i.e., the change in phase of the evenly distributed groups of alternating P_x. (c), (d) Bar graphs show the distribution of phases about the mean value, $\delta\phi$, from the fit with the corresponding width σ.

gyromagnetic ratio lead to very weak signals; also NSE signals could not be obtained at the high B_0 field required to obtain the cross-calibration NMR frequency of 25.6 kHz chosen to reach high enough signal-to-noise ratio. Therefore ^{131}Xe polarization was calibrated in a separate measurement after the NSE experiment, leaving the SEOP apparatus and conditions unchanged. Using an NMR coil with a six-fold higher quality factor, the NMR calibration was performed with a maximum $\pi/2$ tip angle for both Xe isotopes, so one factor of the ratio of gyromagnetic ratios drops out of the calibration calculation. Additionally one needs to account for the ratio of the different nuclear spins. The relation for the calibration ^{131}Xe to ^{129}Xe becomes

$$P_{131}N_{131} = P_{129}N_{129}\left(\frac{\gamma_{129}}{\gamma_{131}}\right)\left(\frac{I_{129}}{I_{131}}\right)\frac{S'_{131}}{S'_{129}}, \tag{5}$$

where S'_x denote the signals obtained for the $\pi/2$ tip angles used for this step. The result is $P_{131}N_{131} = 0.0498P_{129}N_{129} = 8.1 \pm 0.2 \times 10^{22}$ m^{-3}. Given the 0.20 bar total Xe pressure, $P_{131} = 1.96\%$. Neither the specific number densities nor the isotopic concentrations of the xenon isotopes are needed for the neutron scattering length determination with our method using calibrated NMR.

We also briefly measured b_i^3 to compare with previous results. This measurement is calibrated absolutely from the polarization dependent ^{3}He neutron absorption cross section [66]. Our value of $2.280 \pm 0.020(\text{stat.}) + 0.015(\text{syst.})$ fm for b_i^3 agrees with previous work [51,67] and is determined with much higher precision than our b_i values for ^{131}Xe and ^{129}Xe.

Combining Eqs. (2), (3), and (4) or Eq. (5), we can write the magnitudes of incoherent scattering lengths for the xenon isotopes in terms of directly measured experimental quantities as

$$b_i^{129} = \frac{\sqrt{3}}{2}\left(\frac{\gamma_{129}}{\gamma_3}\right)^2 \frac{\phi_{129}}{\cosh^{-1}(R)}\frac{d_3}{d_{129}}\frac{S_3V_{129}}{S_{129}V_3}\frac{\sigma_p}{\lambda_{th}} \tag{6}$$

and

$$b_i^{131} = \frac{3}{2}\sqrt{\frac{5}{3}}\frac{|\gamma_{129}\gamma_{131}|}{\gamma_3^2}\frac{\phi_{131}}{\cosh^{-1}(R)}\frac{d_3}{d_{131}}\frac{S_3V_{129}}{S_{129}V_3}\frac{S'_{129}}{S'_{131}}\frac{\sigma_p}{\lambda_{th}}, \tag{7}$$

where for example $\cosh^{-1}(R) = 0.6939 \pm 0.0040$ for the pixels in the center of the ^{3}He cell. As stated before, we used a previous estimate of $\sigma_1 = 24$ barn [62,67] to determine σ_p and obtain $\lambda P_3 N_3 d_3$ from the ^{3}He cell polarized/unpolarized neutron transmission ratio R [Eq. (3)]. Because the absolute NMR calibration was done with the same neutron beam, the neutron wavelength drops out of the final equations and the b_i values are independent of the detailed shape or mean value of the neutron wavelength distribution. We include the effect of σ_1 as a one-sided systematic error. Other possible corrections due to cell geometry or neutron wavelength distribution shift because of the ^{3}He wavelength-dependent absorption [51] are negligible and are discussed in a related work on b_1^3 [66].

The values of the incoherent scattering lengths are thus

$$b_i^{129} = -0.186 \pm (0.021)_{\text{stat.}} \pm (0.004)_{\text{syst.}}\text{fm}$$

and

$$b_i^{131} = 2.09 \pm (0.29)_{\text{stat.}} \pm (0.12)_{\text{syst.}}\text{fm}.$$

Signs of the scattering lengths are determined from the spin directions in the SEOP setup. The statistical errors 10% and 12% for ^{129}Xe and ^{131}Xe, respectively, come from the scatter of the phase shift fits shown in Fig. 2. These values for b_i are in line with those of other nuclei. We are not aware of any simple argument that can explain why $|b_i^{131}|$ is a factor of 11 larger than $|b_i^{129}|$, but it is known that poorly characterized subthreshold resonances can influence b_i [68]. A summary of the statistical and systematic errors are given in Table I.

With $b_i(^{129}\text{Xe})$ measured in this work, one could probe the degree of entanglement of polarized ^{129}Xe spins generated in atomic collisions in SEOP systems using polarized, mode-entangled neutron beams to measure spin-spin correlation functions as entanglement witnesses for the xenon spin states. A recently developed quantitative theory for the scattering of mode-entangled neutron beams from spin-correlated dimers [69] can be extended to polarized xenon gas, which can be accurately modeled as an ideal gas with an analytical expression for the neutron dynamic structure factor. SEOP collisions of $I = 1/2$ ^{3}He and ^{129}Xe atoms with properly prepared polarized alkali atoms can generate a calculable degree of entanglement in the nuclear spins under certain conditions according to recent work [16,17]. The resulting long-lived entanglement in the nuclear spin system is of interest for optical quantum memories [70–72]. The quantum decoherence of mode-entangled neutron beams passing through dense matter is so small that the measurement of neutron entanglement witnesses for Bell and GHZ inequalities are unaffected [73–75]. The transverse spatial separation between the two opposite-spin sub-beams created in devices like neutron

Wollaston prisms coincides with the range of mean free paths of the polarized ^{129}Xe gas atoms accessible in SEOP cells.

Polarized ^{131}Xe nuclei could be used in a search for new sources of time reversal (T) violation in neutron-nucleus interactions. T violation from some new interaction beyond the standard model of particles and interactions is one of the highest intellectual priorities in nuclear/particle/astrophysics, and could shed light on the matter-antimatter asymmetry in the universe according to the Sakharov argument [76]. The forward scattering amplitude of polarized neutrons in a polarized nuclear target can possess a parity (P)-odd and T-odd term of the form $\vec{s}_n \cdot (\vec{k}_n \times \vec{I})$ where $\vec{s}_n$ is the neutron spin, $\vec{k}_n$ is the neutron momentum, and $\vec{I}$ is the nuclear polarization. Compound neutron-nucleus resonance reactions are known to greatly amplify parity violation in neutron-nucleus interactions [77,78]. A 4% P-odd asymmetry was measured in the 3.2 eV p-wave resonance in ^{131}Xe, an amplification compared to nucleon-nucleon P-odd amplitudes of almost 10^6. The theory that successfully predicted this phenomenon long ago [79,80] implies that P-odd and T-odd interactions between nucleons beyond the standard model should also be amplified by a similar factor [81–83]. Neutron transmission measurements involving such coherent neutron-nucleus interactions could provide null tests for time-reversal invariance that are free from contamination by final state interactions [84]. Advances in neutron polarization technology and source brightness added to progress in SEOP polarization of ^{131}Xe suffice to conduct a sensitive laboratory search for axion-like particle (ALP) exchange [83] to complement astrophysical bounds [85]. ALPs are poorly constrained by EDM searches for ALP masses above 10 meV [86] because the standard model axion relation between axion mass and coupling constant does not apply [87].

H.L. and W.M.S. acknowledge support from US National Science Foundation (NSF) Grants No. PHY-1913789 and No. PHY-2209481 and the Indiana University Center for Spacetime Symmetries. H.L. received a Short-Term Grant, 2019 No. 57442045 from DAAD the German Academic Exchange Service. D.B. and B.M.G. acknowledge support from the NSF (CHE-1905341), DoD (W81XWH-15-1-0272, W81XWH2010578), and a Cottrell Scholar SEED Award from Research Corporation for Science Advancement, and thank T. Gafar, C. Kraft, L. Korando, and A. Ruffing for shipment of the SEOP cells. We acknowledge G. M. Schrank for discussions and M. Huber for detailed discussions of NIST work on b_i^3 and estimates of σ_1 for ^{3}He.

Appendix. As stated in the main paper the ^{129}Xe cell magnetization was measured using NMR, which was calibrated to an absolute ^{3}He standard from neutron transmission during the NSE measurements. The transmission ratio R used to determine P_3N_3 often uses a simplification, namely that $\sigma_{un} \simeq \sigma_p$, i.e., the neutron absorption cross section of the polarized ^{3}He cell, σ_p, is the same as the well-known unpolarized ^{3}He neutron absorption cross section σ_{un}. This approximation can be used to determine the neutron polarization parameters exactly [61], however this is not the case for a precision measurement of P_3. More precisely, $\sigma_p = (1 - \sigma_1/\sigma_{un})\sigma_{un}$ is the polarized ^{3}He spin-dependent neutron absorption cross section, where σ_1, the absorption cross section for the n-^{3}He spin with parallel (i.e., triplet state), is $\neq 0$. Since σ_p is smaller than σ_{un} by σ_1, if one assumes the estimated $\sigma_1 = 24$ barn of Huber *et al.* [62,67] the value of P_3N_3 changes by -0.45% compared to the value using the approximation $\sigma_p \simeq \sigma_{un} = 5333 \pm 7$ barn. We used this estimated value of $\sigma_1 = 24$ barn to correct our reported values of b_i but include its effect on the value of P_3 in the systematic error estimates.

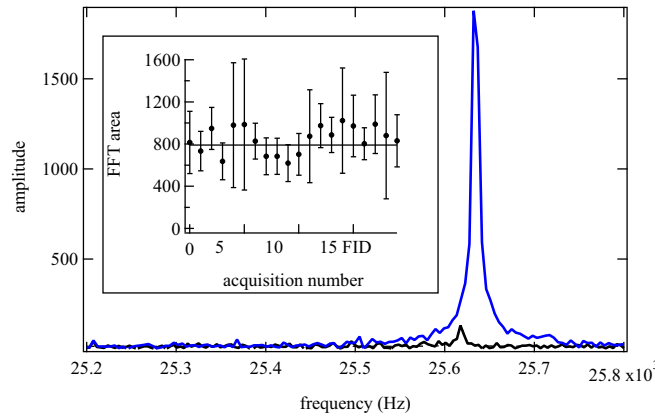

FIG. 3. Example NMR spectra from Fourier-transformed single-shot FID signals utilizing maximum $\pi/2$ excitation amplitude recorded for calibration of the ^{131}Xe cell. ^{131}Xe and ^{129}Xe spectra are black and blue, respectively. The inset shows the NMR FID strengths versus acquisition number used for the averaging of the ^{131}Xe signal.

NMR FID intensity from $P_{129}N_{129}$ was calibrated directly to the FID signal intensity from P_3N_3 utilizing low amplitude excitations (i.e., $\ll \pi/2$) during the NSE measurements. The data were acquired with a home-built single-coil pulse-receive FID system using a 300-turn $D = 2$ cm resonant surface coil (quality factor $\simeq$ 3–4 and all digital signal processing of the raw FID data [60]. Areas of the corresponding FFTs of the digitally mixed-down and filtered FIDs were used to compare the signal strengths at the same NMR frequency. The $P_{131}N_{131}$ to $P_{129}N_{129}$ NMR calibration was performed after the NSE measurements because the B_{SEOP} field required for ^{131}Xe NMR was too high and the resulting FID amplitudes too weak to perform during the NSE measurements. These measurements were performed utilizing a pickup coil with a six-fold higher quality factor, resulting in correspondingly higher FID amplitudes and calibrated $\pi/2$ FID excitation pulses to maximize the small signal from the ^{131}Xe. The $\pi/2$ tipping-pulse strength was determined by maximizing the FID signal strength for saturated Xe polarizations by varying the excitation amplitude. The ratio of the tipping amplitudes V_{131}/V_{129} required for these $\pi/2$ excitations scaled as $\gamma_{129}/\gamma_{131}$ as expected. These single-shot FID strengths were averaged to obtain the saturation $P_{131}N_{131}$ value of our SEOP system and ^{131}Xe cell via the cross calibration to the saturation value of $P_{129}N_{129}$ for our system and the ^{129}Xe cell determined during the NSE measurements. All optical pumping parameters where held constant for the NSE measurements and the later ^{131}Xe NMR calibration. Examples of the ^{129}Xe to ^{131}Xe NMR calibration data are shown in Fig. 3.

[1] L. Van Hove, Phys. Rev. **95**, 249 (1954).
[2] S. W. Lovesey, *Theory of Neutron Scattering from Condensed Matter* (Oxford University Press, New York, 1984), Vol. 2.
[3] R. I. Schermer and M. Blume, Phys. Rev. **166**, 554 (1968).
[4] T. G. Walker and W. Happer, Rev. Mod. Phys. **69**, 629 (1997).
[5] B. Driehuys, G. D. Cates, E. Miron, K. Sauer, D. K. Walter, and W. Happer, Appl. Phys. Lett. **69**, 1668 (1996).
[6] M. S. Rosen, T. E. Chupp, K. P. Coulter, R. C. Welsh, and S. D. Swanson, Rev. Sci. Inst. **70**, 1546 (1999).
[7] A. L. Zook, B. B. Adhyaru, and C. R. Bowers, J. Magn. Reson. **159**, 175 (2002).
[8] M. G. Mortuza, S. Anala, G. E. Pavlovskaya, T. J. Dieken, and T. Meersmann, J. Chem. Phys. **118**, 1581 (2003).
[9] I. C. Ruset, S. Ketel, and F. W. Hersman, Phys. Rev. Lett. **96**, 053002 (2006).
[10] P. Nikolaou, A. M. Coffey, L. L. Walkup, B. M. Gust, N. Whiting, H. Newton, S. Barcus, I. Muradyan, M. Dabaghyan, G. D. Moroz *et al.*, Proc. Natl. Acad. Sci. USA **110**, 14150 (2013).
[11] P. Nikolaou, A. M. Coffey, M. J. Barlow, M. S. Rosen, B. M. Goodson, and E. Y. Chekmenev, Anal. Chem. **86**, 8206 (2014).
[12] G. Norquay, G. J. Collier, M. Rao, N. J. Stewart, and J. M. Wild, Phys. Rev. Lett. **121**, 153201 (2018).
[13] M. Gatzke, G. D. Cates, B. Driehuys, D. Fox, W. Happer, and B. Saam, Phys. Rev. Lett. **70**, 690 (1993).
[14] K. Sauer, R. Fitzgerald, and W. Happer, Chem. Phys. Lett. **277**, 153 (1997).
[15] M. Haake, B. Goodson, D. Laws, E. Brunner, M. Cyrier, R. Havlin, and A. Pines, Chem. Phys. Lett. **292**, 686 (1998).
[16] O. Katz, R. Shaham, and O. Firstenberg, PRX Quantum **3**, 010305 (2022).
[17] O. Katz, R. Shaham, E. Reches, A. V. Gorshkov, and O. Firstenberg, Phys. Rev. A **105**, 042606 (2022).
[18] B. M. Goodson, J. Magn. Reson. **155**, 157 (2002).
[19] Y. Zheng, G. W. Miller, W. A. Tobias, and G. D. Cates, Nature (London) **537**, 652 (2016).
[20] J. P. Mugler III and T. A. Altes, J. Magn. Reson. Imag. **37**, 313 (2013).
[21] A. Khan, R. Harvey, J. Birchall, R. Irwin, P. Nikolaou, G. Schrank, K. Emami, A. Dummer, M. Barlow, B. Goodson *et al.*, Angew. Chem. Int. Ed. **60**, 22126 (2021).
[22] D. A. Barskiy, A. M. Coffey, P. Nikolaou, D. M. Mikhaylov, B. M. Goodson, R. T. Branca, G. J. Lu, M. G. Shapiro, V.-V. Telkki, V. V. Zhivonitko *et al.*, Chem. Eur. J. **23**, 725 (2017).
[23] Z. Wu, W. Happer, and J. M. Daniels, Phys. Rev. Lett. **59**, 1480 (1987).
[24] Z. Wu, S. Schaefer, G. D. Cates, and W. Happer, Phys. Rev. A **37**, 1161 (1988).
[25] D. Raftery, H. Long, T. Meersmann, P. J. Grandinetti, L. Reven, and A. Pines, Phys. Rev. Lett. **66**, 584 (1991).
[26] S. Appelt, G. Wäckerle, and M. Mehring, Phys. Rev. Lett. **72**, 3921 (1994).
[27] D. Bear, R. E. Stoner, R. L. Walsworth, V. A. Kostelecky, and C. D. Lane, Phys. Rev. Lett. **85**, 5038 (2000).
[28] F. Cane, D. Bear, D. F. Phillips, M. S. Rosen, C. L. Smallwood, R. E. Stoner, R. L. Walsworth, and V. A. Kostelecky, Phys. Rev. Lett. **93**, 230801 (2004).
[29] C. Gemmel, W. Heil, S. Karpuk, K. Lenz, Y. Sobolev, K. Tullney, M. Burghoff, W. Kilian, S. Knappe-Gruneberg, W. Muller *et al.*, Phys. Rev. D **82**, 111901(R) (2010).
[30] F. Allmendinger, W. Heil, S. Karpuk, W. Kilian, A. Scharth, U. Schmidt, A. Schnabel, Y. Sobolev, and K. Tullney, Phys. Rev. Lett. **112**, 110801 (2014).
[31] Y. V. Stadnik and V. V. Flambaum, Eur. Phys. J. C **75**, 110 (2015).
[32] V. A. Kostelecky and A. J. Vargas, Phys. Rev. D **98**, 036003 (2018).
[33] F. Allmendinger, I. Engin, W. Heil, S. Karpuk, H.-J. Krause, B. Niederländer, A. Offenhäusser, M. Repetto, U. Schmidt, and S. Zimmer, Phys. Rev. A **100**, 022505 (2019).
[34] N. Sachdeva, I. Fan, E. Babcock, M. Burghoff, T. E. Chupp, S. Degenkolb, P. Fierlinger, S. Haude, E. Kraegeloh, W. Kilian *et al.*, Phys. Rev. Lett. **123**, 143003 (2019).
[35] M. Bulatowicz, R. Griffith, M. Larsen, J. Mirijanian, C. B. Fu, E. Smith, W. M. Snow, H. Yan, and T. G. Walker, Phys. Rev. Lett. **111**, 102001 (2013).
[36] Y.-K. Feng, D.-H. Ning, S.-B. Zhang, Z.-T. Lu, and D. Sheng, Phys. Rev. Lett. **128**, 231803 (2022).
[37] V. Gudkov and H. M. Shimizu, Phys. Rev. C **102**, 015503 (2020).
[38] V. F. Sears, *Neutron Optics: An Introduction to the Theory of Neutron Optical Phenomena and Their Applications* (Oxford University Press, New York, 1989).
[39] V. Baryshevsky and M. Podgoretsky, Zh. Eksp. Teor. Fiz. **47**, 1050 (1964).
[40] A. Abragam and M. Goldman, *Nuclear Magnetism Order and Disorder* (Clarendon Press, Oxford, 1982).
[41] A. G. Klein and S. A. Werner, Rep. Prog. Phys. **46**, 259 (1983).
[42] J. Byrne, *Neutrons, Nuclei, and Matter: An Exploration of the Physics of Slow Neutrons* (Institute of Physics Publishing, Philadelphia, 1994).
[43] P. Chieux and H. Dachs, *Neutron Diffraction*, Lecture Notes in Economic and Mathematical Systems (Springer-Verlag, Berlin, 1978).
[44] N. F. Ramsey, *Molecular Beams* (Oxford University Press, Oxford, 1956).
[45] N. F. Ramsey, Rev. Mod. Phys. **62**, 541 (1990).
[46] A. Abragam, G. Bacchella, H. Glätti, P. Meriel, M. Pinot, and J. Piesvaux, Phys. Rev. Lett. **31**, 776 (1973).
[47] M. Forte, Nuov Cim. A **18**, 726 (1973).
[48] V. G. Pokazanev and G. V. Skrotskii, Phys.-Usp. **22**, 943 (1979).
[49] M. I. Tsulaia, Phys. At. Nucl. **77**, 1321 (2014).
[50] F. Mezei, Z. Phys. A: Hadrons Nucl. **255**, 146 (1972).
[51] O. Zimmer, G. Ehlers, B. Farago, H. Humblot, W. Ketter, and R. Scherm, EPJ Direct **4**, 1 (2002).
[52] E. L. Hahn, Phys. Rev. **80**, 580 (1950).
[53] Heinz Maier-Leibnitz Zentrum *et al.*, J. of Large-Scale Res. Facilities **1**, A11 (2015).
[54] B. Farago and F. Mezei, Physica B+C **136**, 100 (1986).
[55] R. Gähler, R. Golub, and T. Keller, Phys. B: Condens. Matter **180–181**, 899 (1992).
[56] S. Pasini, O. Holderer, T. Kozielewski, D. Richter, and M. Monkenbusch, Rev. Sci. Instrum. **90**, 043107 (2019).
[57] D. R. Rich, S. Fan, T. R. Gentile, D. Hussey, G. L. Jones, B. Neff, W. M. Snow, and A. K. Thompson, Phys. B: Condens. Matter **305**, 203 (2001).
[58] Z. Salhi, E. Babcock, P. Pistel, and A. Ioffe, J. Phys.: Conf. Ser. **528**, 012015 (2014).
[59] M. Molway, L. Bales-Shaffer, K. Ranta, D. Basler, M. Murphy, B. Kidd, A. Gafar, J. Porter, K. Albin, B. Goodson *et al.*, arXiv:2105.03076.

[60] E. Babcock, Z. Salhi, T. Theisselmann, D. Starostin, J. Schmeissner, A. Feoktystov, S. Mattauch, P. Pistel, A. Radulescu, and A. Ioffe, J. Phys.: Conf. Ser. **711**, 012008 (2016).
[61] T. R. Gentile, P. J. Nacher, B. Saam, and T. G. Walker, Rev. Mod. Phys. **89**, 045004 (2017).
[62] M. G. Huber, M. Arif, W. C. Chen, T. R. Gentile, D. S. Hussey, T. C. Black, D. A. Pushin, C. B. Shahi, F. E. Wietfeldt, and L. Yang, arXiv:1409.8567v2.
[63] T. Chupp, K. Coulter, M. Kandes, M. Sharma, T. Smith, G. L. Jones, W. Chen, T. Gentile, D. Rich, B. Lauss *et al.*, Nucl. Instrum. Methods Phys. Res. A **574**, 500 (2007).
[64] R. A. Campbell, H. P. Wacklin, I. Sutton, R. Cubitt, and G. Fragneto, Eur. Phys. J. Plus **126**, 107 (2011).
[65] K. F. Stupic, Z. I. Cleveland, G. E. Pavlovskaya, and T. Meersmann, J. Magn. Reson. **208**, 58 (2011).
[66] H. Lu, O. Holderer, A. Ioffe, S. Pasini, P. Pistel, Z. Salhi, B. M. Goodson, W. M. Snow, and E. Babcock, Phys. Rev. C **108**, L031001 (2023).
[67] M. G. Huber, M. Arif, W. C. Chen, T. R. Gentile, D. S. Hussey, T. C. Black, D. A. Pushin, C. B. Shahi, F. E. Wietfeldt, and L. Yang, Phys. Rev. C **90**, 064004 (2014).
[68] T. Okudaira, R. Nakabe, S. Endo, H. Fujioka, V. Gudkov, I. Ide, T. Ino, M. Ishikado, W. Kambara, S. Kawamura *et al.*, arXiv:2105.03076.
[69] A. A. M. Irfan, P. Backstone, R. Pynn, and G. Ortiz, New J. Phys. **23**, 083022 (2021).
[70] A. Dantan, G. Reinaudi, A. Sinatra, F. Laloe, E. Giacobino, and M. Pinard, Phys. Rev. Lett. **95**, 123002 (2005).
[71] O. Katz, R. Shaham, and O. Firstenberg, Sci. Adv. **7**, eabe9164 (2021).
[72] O. Katz, R. Shaham, E. S. Polzik, and O. Firstenberg, Phys. Rev. Lett. **124**, 043602 (2020).
[73] J. Shen, S. Kuhn, D. Baxter, R. Dalgleish, F. Li, S. Lu, G. Ortiz, J. Plomp, S. Parnell, R. Pynn *et al.*, Nat. Commun. **11**, 930 (2020).
[74] S. Lu, A. A. Md. Irfan, J. Shen, S. J. Kuhn, W. M. Snow, D. V. Baxter, R. Pynn, and G. Ortiz, Phys. Rev. A **101**, 042318 (2020).
[75] S. J. Kuhn, S. McKay, J. Shen, N. Geerits, R. M. Dalgliesh, E. Dees, A. A. M. Irfan, F. Li, S. Lu, V. Vangelista *et al.*, Phys. Rev. Res. **3**, 023227 (2021).
[76] A. D. Sakharov, Pisma Zh. Eksp. Teor. Fiz **5**, 32 (1967).
[77] G. E. Mitchell, J. D. Bowman, and H. A. Weidenmüller, Rev. Mod. Phys. **71**, 445 (1999).
[78] G. Mitchell, J. Bowman, S. Penttila, and E. Sharapov, Phys. Rep. **354**, 157 (2001).
[79] O. P. Sushkov and V. V. Flambaum, JETP Lett. **32**, 352 (1980).
[80] O. P. Sushkov and V. V. Flambaum, Sov. Phys. Usp. **25**, 1 (1982).
[81] V. R. Bunakov and V. Gudkov, Z. Phys. A **308**, 363 (1982).
[82] V. Gudkov, Nucl. Phys. A **524**, 668 (1991).
[83] P. Fadeev and V. V. Flambaum, Phys. Rev. C **100**, 015504 (2019).
[84] J. D. Bowman and V. Gudkov, Phys. Rev. C **90**, 065503 (2014).
[85] G. Raffelt, Phys. Rev. D **86**, 015001 (2012).
[86] V. A. Dzuba, V. V. Flambaum, I. B. Samsonov, and Y. V. Stadnik, Phys. Rev. D **98**, 035048 (2018).
[87] S. Mantry, M. Pitschmann, and M. J. Ramsey-Musolf, Phys. Rev. D **90**, 054016 (2014).